

Microstructure and dynamic mechanical properties of magnetorheological elastomer based on ethylene/acrylic elastomer prepared using different manufacturing methods

Tianming Gao^{1,2}, Ruihong Xie², Kyungho Chung¹ ✉

¹Department of Polymer Engineering, The University of Suwon, Hwaseong-Si, Gyeonggi-Do 445743, Republic of Korea

²Agricultural Product Processing Research Institute, Chinese Academy of Tropical Agriculture Science, Zhanjiang 524001, People's Republic of China

✉ E-mail: khchung@suwon.ac.kr

Published in Micro & Nano Letters; Received on 4th June 2017; Revised on 14th March 2018; Accepted on 4th April 2018

Magneto-rheological elastomer (MRE) is a kind of smart material based on elastomer matrix and it is divided into isotropic (i-MRE) and anisotropic MRE (a-MRE) depending on the magnetic particle arrangement. In the i-MRE, carbonyl iron particles (CIP) are randomly dispersed, while they form a chain-like structure in the a-MRE. Two manufacturing procedures of a-MRE have been introduced. The a-MRE-1 was manufactured by one-step process involving application of magnetic field and curing of matrix simultaneously. On the other hand, a-MRE-2 was manufactured by two-step process in which the magnetic field was applied to induce CIP orientation and then the matrix was cured. The microstructure and mechanical properties of MRE were characterised by scanning electron microscope, universal testing machine and dynamic mechanical analysis. The results showed that the CIP content in MRE had no effect on the cure properties. A chain-like structure existed in a-MRE-1, whereas the orientation structure of CIP in the a-MRE-2 was not as clear as that in a-MRE-1. The tensile strength of a-MRE-1 was the lowest because no interfacial reaction occurred between the CIP and the rubber molecules chain, whereas i-MRE had the highest tensile strength.

1. Introduction: A magnetorheological (MR) material is a type of functional and smart material which has rheological and dynamic properties that can be stimulated by an external magnetic field [1, 2]. Since the discovery of MR effect by Rabinow [3], most researchers have paid more attention to MR fluids, MR foams, and MR elastomers (MRE) [4, 5]. MRE is a type of smart composite containing elastomer and magnetic particles. MRE have been applied widely as damping components [6], shock absorbers [7], noise barrier systems [8], isolators [9], and magneto-resistor sensors [10, 11], because they show excellent strain and MR effects when stimulated under an external magnetic field. Over the past decade, MRE have attracted considerable interest, and many types of elastomers have been prepared as MRE [12–20].

In general, MRE can be classified into two categories, isotropic and anisotropic MRE depending on the orientation of the magnetic particles [21]. In contrast to the random dispersion of carbonyl iron particles (CIP) in the isotropic MRE, the magnetic particles have a chain-like structure and are locked in the elastomer matrix after pre-forming under magnetic field and curing processing in the anisotropic MRE. Therefore, magnetic processing for the magnetic particle orientation and curing to lock the magnetic particles in an elastomer matrix are essential procedures for the preparation of MRE.

Over the past decade, there have been mainly two different manufacturing methods for anisotropic MRE preparation. One was pre-forming a configuration of CIP and curing compound simultaneously (for short: one-step); and another was to place the sample into the mould under a magnetic field for pre-forming, followed by curing the orientation sample at the curing temperature (for short: two-step). Ge *et al.* [22] treated the compound under a magnetic field, and then shut the magnetic field down and further increased the temperature to cure the samples. Liao *et al.* [23] prepared MRE based on the silicone rubber by two-step manufacturing method. Khimi *et al.* [14] prepared MRE based on the natural rubber (NR), and the compound was subjected to a magnetic field at 80°C for 30 min, and then was cured at 150°C. With the exception of the two-step method mentioned before, some researchers placed the compound into a mould, applied a magnetic field, and simultaneously cured it at the curing temperature [5, 24].

However, the effects of different manufacturing methods on the microstructure and dynamic properties have not been reported.

Ethylene/acrylic elastomer (AEM) was introduced commercially in 1975 by the Du Pont Company under the trademark, Vamac[®] [25]. Owing to its good low-temperature properties and excellent resistance to compression setting and the combined deteriorating influences of heat, oil, and weather, it has been used in automobile industries as seals, gaskets and torsional vibration dampers [26, 27]. In addition, the Mooney viscosity of AEM is about 20, which is lower compared to natural rubber (Mooney viscosity about 60). Hence, the CIP is easy to move in the matrix compare to higher Mooney viscosity elastomer.

In this Letter, two different manufacturing methods (one-step and two-step manufacturing) were used to prepare MRE based on AEM and the microstructure and dynamic properties were characterised. The dynamic properties and morphology of MRE manufactured by different methods were examined by modified dynamic thermo-mechanical analysis (DMA) and scanning electron microscopy (SEM). Finally, according to the morphology, the effects of the dynamic properties manufactured on different methods were analysed and a mechanism was proposed.

2. Experimental

2.1. Materials: AEM (type G, Mooney viscosity: 16.5) was purchased from DUPONT Packaging & Industrial Polymers, Wilmington, DE, USA. Carbon black, N330, was supplied by Aditya Birla Chemicals Co., Ltd., Korea. The magnetic particles, CIP, were provided by BASF in Germany with an approximate size of 3–5 µm and a density of 7.8 g/cm³. The other agents were commercial products.

2.2. Preparation of MRE based on AEM: In order to prepare the MRE, 100phr AEM, 30phr CB, 1.5phr polyoxyethylene octadecyl ether phosphate, 4.0phr 1,3-di-*O*-tolylguanidine, and 1.5phr hexamethylene diamine carbamate (Diak No. 1) were used. The volume fraction of CIP was 0, 10, 20, 30, and 40 vol. %, respectively.

i-MRE and a-MRE were fabricated by different methods as follows.

Isotropic MRE (i-MRE): the rubber compounds were placed into a hydraulic hot press at 165°C for 20 min.

Anisotropic MRE manufactured by one-step process (a-MRE-1): the rubber compounds were placed into a mould for pre-forming under an external magnetic field of 1300 mT and sufficient pressure, generated by the designed magnet-heat couple machine at 165°C for 15 min, and simultaneously cured at 165°C for 20 min.

Anisotropic MRE manufactured by two-step process (a-MRE-2): the rubber compounds were placed into a mould for pre-forming under an external magnetic field of 1300 mT and sufficient pressure, which were generated by a magnet-heat coupled machine at 100°C for 15 min. The temperature was then increased to 165°C, and the curing procedure was performed at 165°C for 20 min.

The magnet-heat coupled machine was composed of a magnetic field, a mould, and a controllable heating system, as illustrated in Fig. 1.

2.3. Measurement and characterisation

2.3.1. Curing characterisation: The curing characterisation of MRE based on the AEM, including the scorch time (t_{s2}), optimal cure time (t_{90}), minimum torque (M_L), and maximum torque (M_H), was determined using a DRM-100 Rheometer (Daekyung Engineering, Korea) at 165°C. The cure rate index (CRI) was employed to evaluate the cure rate of the rubber compounds, which was calculated as

$$CRI = \frac{100}{t_{90} - t_{s2}} \quad (1)$$

2.3.2. Morphology: The morphology of MRE was characterised by SEM (JSM-7800F, JEOL, Japan). The accelerating voltage was set to 15 kV. Before the SEM observations, the AEM/CIP composite samples that had been pretreated with liquid nitrogen and freeze-fractured were coated with a thin gold layer to avoid surface charging.

2.3.3. Mechanical properties: The mechanical properties (tensile strength and elongation at break) were measured using a universal testing machine (DUT-500CM, Daekyung Engineering Co. Ltd, Korea) with a crosshead speed of 500 mm/min according to ASTM D412-06a. Five pieces of each sample were tested, and the mean value was obtained.

2.3.4. Dynamic mechanical analysis: DMA (Mettler Toledo Ltd, UK, model SDT861e) was performed to measure the dynamic properties, such as the storage modulus and loss factor, under different magnetic fields. This machine was designed by our group, but was assembled by Daekyung Engineering Co. Ltd, Korea [2]. In the

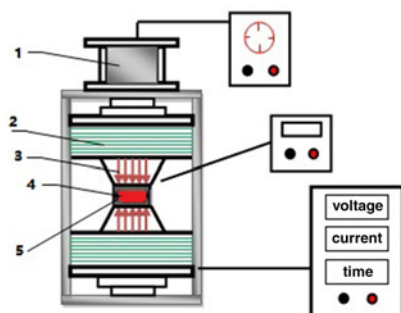


Fig. 1 Graphical representation of the magnetic field and heat curing coupled machine for fabrication of MRE
(1) Hydraulic cylinder, (2) Wire coil, (3) Heater, (4) Sample, (5) Sample mould

experiments, the CIP chain orientation was perpendicular to the direction of the shear stress force. Magnetic field sweep (field range 0 to 1200 mT) measurements were taken at a strain of 1% and a frequency of 1 Hz.

2.3.5. Temperature sweep by rubber process analyser (RPA): The temperature sweep of the compound was performed from 100 to 170°C at 0.5 Hz and 1° strain using an RPA (RPA2000, Alpha Technological, OH, USA).

3. Results and discussion

3.1. Vulcanisation properties: Vulcanisation is very important procedure in elastomer processing [28]. The CIP used in this Letter could be locked in the matrix after vulcanisation. Table 1 shows the vulcanisation characteristics of AEM filled with different CIP contents. As shown in Table 1, the scorch time (t_{s2}) and optimal cure time (t_{90}) of the compound were almost unaffected by the CIP loading. The CRI was in the range between 6.20 and 6.80, hence, the vulcanisation rate was not impacted by the increase in CIP loading based on AEM. On the other hand, the maximum torque (M_H) of MRE increased because of the increased CIP content. The M_H reached 42 dNm when the CIP content was 40 vol.% in the MRE. According to the cure rheograph, the AEM compound showed plateau behavior and the t_{90} was 16.13–17.49 min. Thus, we determined that 20 min was enough time for curing of AEM-based MRE. Even though the curing time is prolonged, AEM will not be decomposed due to its good ageing resistant [25].

3.2. Morphology: Fig. 2 shows the morphology of the isotropic MRE and anisotropic MRE prepared by different methods. The

Table 1 Vulcanisation parameters for the MRE samples with different CIPs contents

CIPs content, vol. %	t_{s2} , min	t_{90} , min	M_H , dNm	M_L , dNm	CRI
0	1.46	17.49	28.2	2.6	6.21
10	1.42	16.13	32.3	4.0	6.80
20	1.27	17.27	33.9	3.3	6.25
30	1.32	17.16	37.5	4.7	6.31
40	1.06	16.44	42.0	5.1	6.50

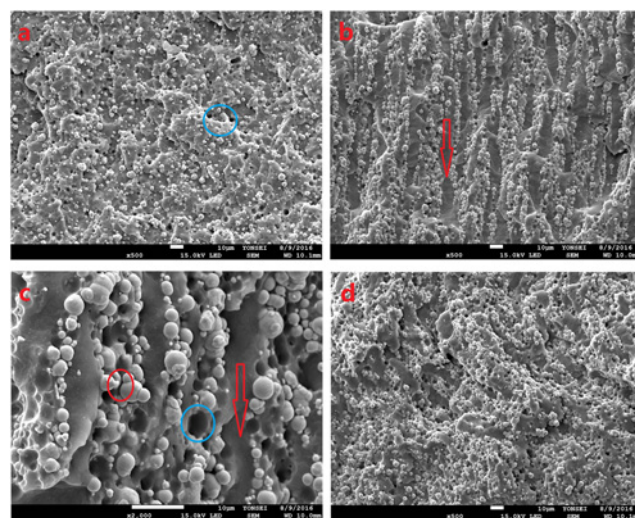


Fig. 2 Morphology of MRE composites with 30 vol.% CIP
a i-MRE
b a-MRE-1 with 500× magnification
c a-MRE-1 with 2000× magnification
d a-MRE-2

dispersion of CIPs in the AEM matrix was uniform and random when no magnetic field was applied during manufacturing, as shown in Fig. 2a. The CIP exhibited an isotropic structure in the MRE based on AEM. Moreover, black holes, marked by a blue circle, were observed in the matrix. The holes were left by the CIP removed during the freeze-fracture process. This shows that there was no interfacial attraction between the CIP and AEM matrix.

Fig. 2b shows the morphology of a-MRE-1 at 500 \times magnification. Owing to the magnetic force, chain-like or columnar structures of CIP were observed in the AEM matrix (represented by the red arrow) and the CIP exhibited anisotropic properties.

Fig. 2c shows the same observation spot as in Fig. 2b but at a 2000 \times magnification. Under a magnetic force, the CIP was aligned parallel to the direction of the magnetic field. The CIP was not aligned as a single particle, but arrayed into a columnar structure containing several aggregated particles. Some gaps were observed among the CIP particles in the MRE, which are marked by the red circle, due to the lack of chemical reactions among the CIP particles. Furthermore, black holes were observed in the matrix, as marked by a blue circle. This shows that no interfacial attraction existed between the CIP and AEM molecular chains.

Fig. 2d shows the morphology of a-MRE-2. Almost no chain-like structures were observed in a-MRE-2. In general, the a-MRE prepared by one-step manufacturing (a-MRE-1) had a better alignment structure than the a-MRE prepared by two-step manufacturing (a-MRE-2).

3.3. Mechanical properties of MRE: Fig. 3 shows the tensile strength and elongation at break of i-MRE, a-MRE-1, and a-MRE-2. The tensile strength of AEM without CIP was 16.32 MPa, whereas, tensile strength of i-MRE, a-MRE-1, and a-MRE-2 containing 40 vol.% of CIP decreased to 8.06, 5.16, and 6.68 MPa, respectively. When the same amount of CIP was filled into the AEM, the tensile strength of a-MRE-2 was higher than that of a-MRE-1. On the other hand, the tensile strength of i-MRE was the highest out of all of the samples. In case of the elongation at break, there was a similar trend with the tensile strength. The elongation at break decreased with increasing CIP loading. The elongation at break of i-MRE was the highest, and elongation at break of a-MRE-1 was lower than that of a-MRE-2.

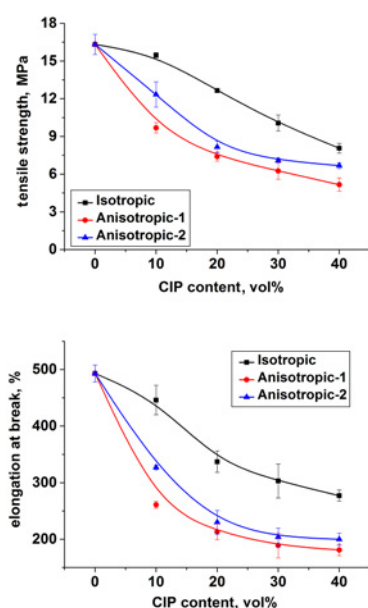


Fig. 3 Tensile strength and elongation at break of i-MRE, a-MRE-1 and a-MRE-2 with different CIP content

As shown in Figs. 2a and b, there was lack of interaction between the CIP particles and AEM matrix, and gaps existed among the CIP particles. The tensile strength and elongation at break decreased with increasing CIP loading. The orientation of filler affects to the mechanical properties of composite, for example, tensile strength of composite with longitudinal orientation of filler is higher than that of composite with transverse orientation [29, 30]. Moreover, there was not interfacial interaction among iron particles. Hence, the perpendicular direction of stretching and the CIP chains resulted in lower tensile strength of a-MRE-1 compared to that of a-MRE-2.

3.4. Dynamic properties

3.4.1. Storage modulus (G'): Fig. 4 shows the storage modulus (G') of the MRE with different CIP contents under different magnetic field intensities. As shown in Fig. 4, the G' of all samples not only increased with increasing external magnetic field intensity, they also increased with increasing CIP content in the MRE matrix. The maximum G' of i-MRE, a-MRE-1, a-MRE-2 were 1.34, 1.61, and 1.44 MPa, respectively, when CIP content was 40 vol.% under the intensity of magnetic field at 1200 mT. Meanwhile, the minimum G' of i-MRE, a-MRE-1, a-MRE-2 was 0.91, 0.92, and 0.91 MPa, respectively, when CIP content was 10 vol.% under no magnetic field. As shown in Fig. 4, the G' of i-MRE was the lowest in all samples when the CIP content was the same in the matrix under identical magnetic field, while the G' of a-MRE-1 was the highest. The G' of a-MRE-2 was higher than that of i-MRE but was lower than that of a-MRE-1.

This phenomenon was caused by the orientation of CIP in the matrix. The a-MRE-1 had good CIP orientation in the matrix, and it resulted in higher G' of MRE. On the other hand, the chain-like

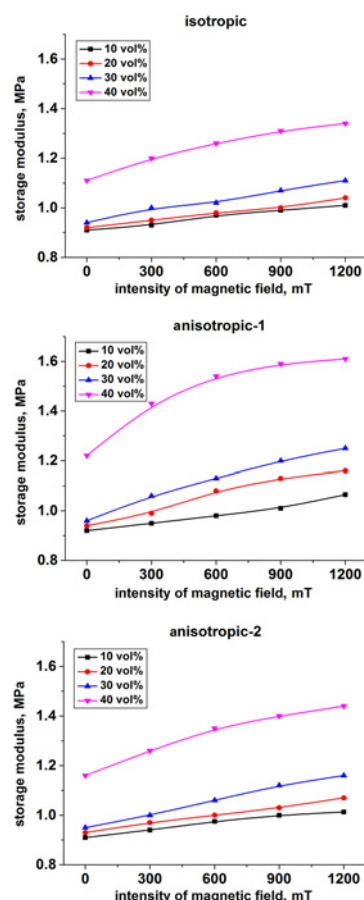


Fig. 4 Storage modulus of i-MRE, a-MRE-1, and a-MRE-2 with different CIP volume content under different intensities of magnetic field

structure of a-MRE-2 was not as good as that of a-MRE-1, hence, the G' of a-MRE-2 was lower than that of a-MRE-1. In general, there were opposite results between mechanical properties and dynamic properties, which caused by different test mode. The direction of mechanical property measurement was perpendicular to CIPs orientation, while the direction of dynamic property measurement was parallel to CIPs orientation. The detailed theory will be discussed in the future work.

3.4.2. MR effect: The MR effect is an important parameter for describing the MR performance, which is expressed as [2, 5]

$$G_{\text{MR-effect}} = \frac{G_T - G_0}{G_0} \times 100\% \quad (2)$$

where G_0 is the initial shear modulus, G_T is the field-induced shear modulus under a variable magnetic field intensity, and $G_{\text{MR-effect}}$ is the MR effect. Fig. 5 shows the MR effect of i-MRE, a-MRE-1, and a-MRE-2 with different CIP contents under a magnetic field of 0 and 1200 mT, where all data were calculated using (2). The results showed that the MR effect increased with increasing CIP content. When the CIP loading increased from 10 to 40 vol.% under the magnetic field of 1200 mT, the MR effect increased from 11 to 21% for i-MRE, 16 to 32% for a-MRE-1, and 12 to 24% for a-MRE-2, respectively. The MR effect of a-MRE-1 was higher than that of a-MRE-2, obviously, because of its good chain-like structure of CIP. It brought about higher storage modulus of MRE under the magnetic field.

3.5. Mechanism of different manufacturing methods: According to SEM results in this work, there was a clear chain-like structure of a-MRE-1, and it had higher MR effect compared to a-MRE-2. On the other hand, a-MRE-1 had a lower tensile strength and elongation at break than a-MRE-2. Fig. 6 shows the relationship of the compound viscosity and CIP content at the temperature sweep. The viscosity of the compound increased with increasing CIP content. The viscosity of the compound showed a U-curve under the temperature sweep; the viscosity decreased until the temperature reached 130°C, at which point the viscosity increased

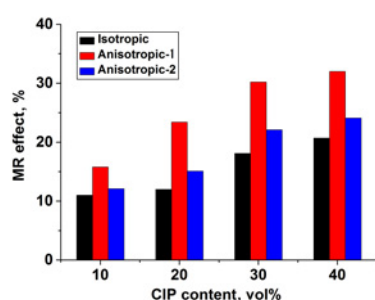


Fig. 5 MR effect of i-MRE, a-MRE-1, and a-MRE-2 with different CIP volume content

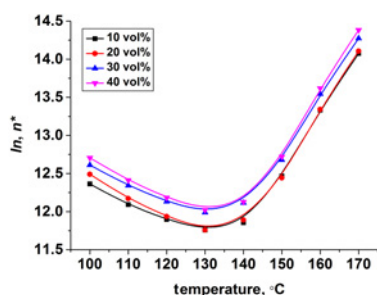


Fig. 6 Relationship of viscosity (logarithm) and temperature for AEM/CB/CIP compound with different CIP loadings (vol.%)

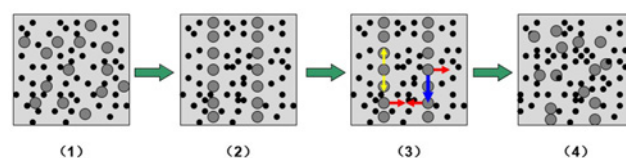


Fig. 7 Scheme of CIP evolution in two-step manufacturing AEM. (Grey particle and black particle represent CIP and carbon black, respectively; blue, red and yellow arrowhead represent gravity, collision force between carbon black and CIP, collision force between CIP and CIP, respectively)

with increasing temperature. The viscosity of an elastomer usually decreases with increasing temperature. However, the viscosity of the compound studied increased due to cross-link material in the AEM matrix, and the cross-link density of MRE increased with increasing temperature. In case of one-step manufacturing process, the magnetisation and curing process are performed simultaneously. Therefore, a chain-like structure is easily obtained in this case.

The compound produced by two-step manufacturing was treated magnetically at 100°C, and the temperature was then increased to the curing temperature (165°C) to cure the MRE under no magnetic field. Based on the SEM image, the CIP particles in a-MRE-2 did not form a chain-like structure as in a-MRE-1. This phenomenon can be explained in three ways. First, the Mooney viscosity of AEM (type G) is 16.5, which is lower than many other kind of rubber, such as natural rubber. With the increasing temperature, viscosity of rubber decreased, and the CIP moved more easily in the matrix. Second, the density of CIP was higher than AEM and carbon black; hence, the CIP particles settled due to the gravity. Third, the particle motion was enhanced by the increase in temperature, such as the force among CIP particles, between CIP and carbon black, and between CIP and the molecular chain of AEM. In general, lower viscosity of AEM, the movement of CIP was enhanced and the viscosity of AEM decreased due to the increase in temperature. Therefore, the chain-like structure had been destroyed (Fig. 7).

4. Conclusion: The MRE was fabricated by two different methods: one-step manufacturing (a-MRE-1) and two-step manufacturing (a-MRE-2) methods. The a-MRE-1 had chain-like structures in the matrix, while but there was no interfacial reaction between the CIP and elastomer. The structural the orientation of CIP in the a-MRE-2 was not as clear as in a-MRE-1. With increasing CIP content, the tensile strength and elongation at break decreased. The tensile strength and elongation at break of a-MRE-1 was the lowest in all of the samples because there was no interfacial reaction between CIP and the elastomer, and the CIP was well oriented. The shear storage modulus and MR effect of i-MREs and a-MREs improved with increasing CIP content, and the MR effect of a-MRE-1 was higher than that of a-MRE-2 at the same intensity of magnetic field. The distinct microstructure, mechanical, and dynamic properties of the MRE prepared by different methods were attributed to the decrease in viscosity, gravity, molecular force between the elastomer molecules and CIP, and interaction force among CIP particles. Overall, the one-step manufacturing is more suitable for the preparation of MRE based on AEM.

5. Acknowledgments: This study was funded by Components and Materials Technology Development (grant no. 10047791) of the Ministry of Trade, Industry and Energy of Korea.

6 Reference

- [1] Feng J.B., Xuan S.H., Liu T.X., ET AL.: 'The prestress-dependent mechanical response of magnetorheological elastomers', *Smart Mater. Struct.*, 2015, **24**, p. 085032

- [2] Wang Y.H., Zhang X.R., Oh J.E., *ET AL.*: 'Fabrication and properties of magnetorheological elastomers based on CR/ENR self-crosslinking blends', *Smart Mater. Struct.*, 2015, **24**, p. 095006
- [3] Rabinow J.: 'The magnetic fluid clutch', *Trans. Am. Inst. Electr. Eng.*, 1948, **67**, pp. 1308–1315
- [4] Claracq J., Sarrazin J., Montfort J.P.: 'Viscoelastic properties of magnetorheological fluids', *Rheol. Acta*, 2004, **43**, pp. 38–49
- [5] Ju B.X., Yu M., Fu J., *ET AL.*: 'A novel porous magnetorheological elastomer: preparation and evaluation', *Smart Mater. Struct.*, 2012, **21**, p. 035001
- [6] Ginder J.M., Schlotter W.F., Nichols M.E.: 'Magnetorheological elastomers in tunable vibration absorbers', *Proc. SPIE 4331, Smart Structures and Materials 2001: Damping and Isolation*, Newport Beach, CA, USA, July 2001, p. 432694
- [7] Sun S.S., Deng H.X., Yang J., *ET AL.*: 'An adaptive tuned vibration absorber based on multilayered MR elastomers', *Smart Mater. Struct.*, 2015, **24**, p. 045045
- [8] Farshad M., Roux M.L.: 'A new active noise abatement barrier system', *Polym. Test.*, 2004, **23**, pp. 855–860
- [9] Yang J., Sun S.S., Du H.P., *ET AL.*: 'A novel magnetorheological elastomer isolator with negative changing stiffness for vibration reduction', *Smart Mater. Struct.*, 2014, **23**, p. 105023
- [10] Tian T.F., Li W.H., Deng Y.M.: 'Sensing capabilities of graphite based MR elastomers', *Smart Mater. Struct.*, 2011, **20**, p. 025022
- [11] Li W.H., Kostidis K., Zhang X.Z., *ET AL.*: 'Development of a force sensor working with MR elastomers'. *IEEE/ASME Int. Conf. Advanced Intelligent Mechatronics (AIM)*, Piscataway, NJ, 233, 2009
- [12] Choi J.Y., Chung K.H.: 'Magnetorheological elastomer based on reactive blend of maleic anhydride grafted chloroprene rubber and epoxidized natural rubber', *Elastom. Compos.*, 2014, **49**, pp. 267–274
- [13] Chung K.H., Jeong U.C., Oh J.E., *ET AL.*: 'Effects of magnetic field input cycle and peptizer on the MR effect of magneto-rheological elastomer based on natural rubber', *Polym. Eng. Sci.*, 2015, **55**, pp. 2669–2675
- [14] Khimi S.R., Pickering K.L.: 'Comparison of dynamic properties of magnetorheological elastomers with existing antivibration rubbers', *Compos. Part B*, 2015, **83**, pp. 175–183
- [15] Jia Y., Jiang Z.M., Gong X.L., *ET AL.*: 'Creep of thermoplastic polyurethane reinforced with ozone functionalized carbon nanotubes', *Express Polym. Lett.*, 2012, **6**, pp. 750–758
- [16] Xu Y.G., Liu T.X., Wu Q., *ET AL.*: 'The energy dissipation behaviors of magneto-sensitive polymer gel under cyclic shear loading', *Mater. Lett.*, 2015, **158**, pp. 406–408
- [17] Choi S.Y., Chung K.H., Kwon S.H., *ET AL.*: 'Effect of surface treated magneto-responsible particle on the property of magneto-rheological elastomer based on silicone rubber', *Elastom. Compos.*, 2016, **51**, pp. 113–121
- [18] Schubert G., Harrison P.: 'Large-strain behaviour of magneto-rheological elastomers tested under uniaxial compression and tension, and pure shear deformations', *Polym. Test.*, 2015, **42**, pp. 122–134
- [19] Yildirim T., Ghayesh M.H., Li W.H., *ET AL.*: 'Experimental nonlinear dynamics of a geometrically imperfect magneto-rheological elastomer sandwich beam', *Compos. Struct.*, 2016, **138**, pp. 381–390
- [20] Qiao X.Y., Lu X.S., Gong X.L., *ET AL.*: 'Effect of carbonyl iron concentration and processing conditions on the structure and properties of the thermoplastic magnetorheological elastomer composites based on poly(styrene-b-ethylene-co-butylene-styrene) (SEBS)', *Polym. Test.*, 2015, **47**, pp. 51–58
- [21] Yoon J.H., Yang I.H., Jeong U.C., *ET AL.*: 'Investigation on variable shear modulus of magnetorheological elastomer based on natural rubber due to change of fabrication design', *Polym. Eng. Sci.*, 2013, **53**, pp. 992–1000
- [22] Ge L., Gong X.L., Fan Y.C., *ET AL.*: 'Preparation and mechanical properties of the magnetorheological elastomer based on natural rubber/rosin glycerin hybrid matrix', *Smart Mater. Struct.*, 2013, **22**, p. 115029
- [23] Liao G.J., Gong X.L., Xuan S.H., *ET AL.*: 'Magnetic-field-induced normal force of magnetorheological elastomer under compression status', *Ind. Eng. Chem. Res.*, 2012, **51**, pp. 3322–3328
- [24] Sorokin V.V., Stepanov G.V., Shamonin M., *ET AL.*: 'Hysteresis of the viscoelastic properties and the normal force in magnetically and mechanically soft magnetoactive elastomers: effects of filler composition, strain amplitude and magnetic field', *Polymer*, 2015, **76**, pp. 191–202
- [25] Babbitt R.O.: 'The Vanderbilt rubber handbook', In Babbitt R.O. (Ed): 'Commercial elastomers and polymers' (R.T. Vanderbilt Company Inc., Norwalk, CT, 1978), p. 262
- [26] McBride E., Dobel T.: 'AEM polymer for seals and gaskets with low oil swell and improved processing', *Rubber World*, 2012, **247**, pp. 29–35
- [27] McBride E.: 'Low volatility plasticizers for AEM compounds', *Rubber World*, 2015, **252**, pp. 32–39
- [28] Gao T.M., Xie R.H., Zhang L.H., *ET AL.*: 'Characterization of the dynamic properties of natural rubbers coagulated using different methods', *Polym. Korea*, 2016, **40**, pp. 446–451
- [29] Geethamma V.G., Thomas M.K., Lakshminarayanan R., *ET AL.*: 'Composite of short coir fibres and natural rubber: effect of chemical modification, loading and orientation of fibre', *Polymer*, 1998, **39**, pp. 1483–1491
- [30] Geethamma V.C., Joseph R., Thomas S., *ET AL.*: 'Short coir fiber-reinforced natural rubber composites: effects of fiber length, orientation, and alkali treatment', *J. Appl. Polym. Sci.*, 1995, **55**, pp. 583–594